

Self-Assembly of 4-(Diethylboryl)pyridine: Crystal Structures of the Cyclic Pentamer and Hexamer and Their Solvent-Dependent Selective Crystallization

Shigeharu Wakabayashi,^{*,†} Yuka Hori,[†] Seiji Komeda,[‡] Yuki Shimizu,[§] Yasuhiro Ohki,[§] Misaki Horiuchi,^{||} Takahito Ito,^{||} Yoshikazu Sugihara,[⊥] and Kazuyuki Tatsumi[#]

[†]Department of Clinical Nutrition, Faculty of Health Science, Suzuka University of Medical Science, Suzuka, Mie 510-0293, Japan

[‡]Department of Pharmaceutical Sciences, Faculty of Pharmaceutical Sciences, Suzuka University of Medical Science, Suzuka, Mie 513-8670, Japan

[§]Department of Chemistry, Graduate School of Science, Nagoya University, Furo-cho, Chikusa-ku, Nagoya 464-8602, Japan

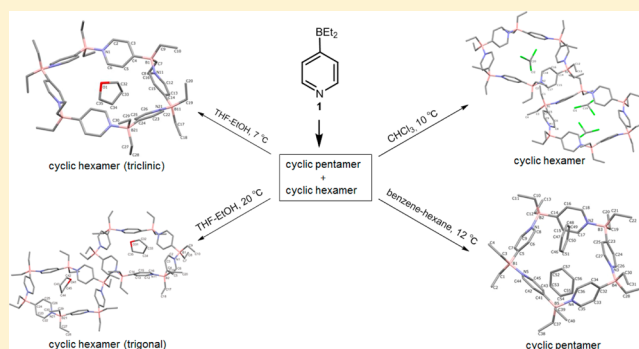
^{||}Division of Chemistry for Materials, Graduate School of Engineering, Mie University, Tsu, Mie 514-8507, Japan

[⊥]Department of Chemistry, Faculty of Science, Yamaguchi University, Yamaguchi 753-8512, Japan

[#]Research Center for Materials Science, Nagoya University, Furo-cho, Chikusa-ku, Nagoya 464-8602, Japan

Supporting Information

ABSTRACT: Two distinct oligomeric structures were obtained by the self-assembly of 4-(diethylboryl)pyridine (**1**). In the ¹H NMR spectrum of **1** in CDCl₃, at least two sets of signals were observed for the pyridyl α- and β-hydrogen atoms. ESI-MS, VPO, and TLC analysis revealed that **1** assembles mainly into a mixture of cyclic pentamers and hexamers in solution via intermolecular boron–nitrogen coordination bonds. Crystallization of **1** in THF by vapor diffusion of EtOH or in CHCl₃ afforded the cyclic hexamer incorporating one THF molecule (I₆·THF) or 1.5 mol equiv of chloroform molecule (I₆·CHCl₃), respectively. Similarly, a solution of **1** in a mixture of benzene and hexane furnished the cyclic pentamer bearing two benzene molecules (I₅·C₆H₆). It seems that the solvent differences affected the crystallization of the two distinct cyclic oligomers of **1**, either of which was cocrystallized predominantly with the solvent molecule. Thermogravimetric analysis of the crystals and NMR studies of the solution revealed that the noncovalent interactions between the host and guest are not strong enough to hold the guest molecule in the cavity.



INTRODUCTION

Organoboranes have drawn significant attention, not only as widely employed reagents in synthetic organic chemistry¹ but also as versatile building blocks in molecular self-assembly.² Our studies on borylpyridines, which contain a boron atom as a coordination center and a pyridine ring as a ligand, revealed that these compounds form the cyclic oligomeric assembly via intermolecular boron–nitrogen coordination bonds.³ Structure construction with a coordination bond plays a critical role in the formation of complex and functional structures for basic research and industrial applications.⁴ Therefore, the extension of our work to novel borylpyridine systems with functionality would be a particularly interesting subject.

Herein, we report the self-assembly of 4-(diethylboryl)pyridine (**1**), the crystal structures of the two assemblies, and the drastic solvent effect in crystallization. Compound **1** assembles into a mixture of cyclic pentamers and hexamers, either of which are selectively cocrystallized with solvent

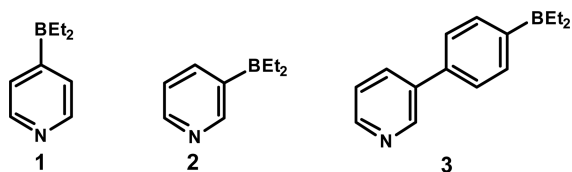
molecules. The ability to obtain pentamer or hexamer crystals appears to be dependent on the solvent used for crystallization. This simple method of selective crystallization is important as a separation technique. The structure elucidation based on NMR, ESI-MS, VPO, and thermogravimetric analysis (TGA) is also provided, and some structural features are compared with 3-(diethylboryl)pyridine (**2**)^{3a} and 3-[4'-(diethylboryl)phenyl]pyridine (**3**).^{3b}

RESULTS AND DISCUSSION

Synthesis. Compound **1** was prepared according to the method described in the literature.⁵ The reaction of 4-bromopyridine with *n*-butyllithium followed by diethylmethoxyborane at -78 °C provided **1** in 68% yield as a colorless solid

Received: December 23, 2015

Published: February 19, 2016



(mp >200 °C). The compound was stable and showed no sign of degradation after storage for 1 year at –20 °C.

NMR Spectroscopy, Mass Spectrometry, and Vapor Pressure Osmometry. In the ^1H NMR spectrum of compound **1** in CDCl_3 , at least two sets of signals were observed for the pyridyl α - and β -hydrogen atoms (Figure S1 in the Supporting Information). The integration values of the ^1H NMR signals were found to differ depending on the sample lot, which implied the existence of at least two species. The TLC analysis also indicated a mixture of at least two species, which would likely be difficult to separate by the usual column chromatography.

ESI-MS measurement of **1** in THF in the presence of LiCl provided charged peaks at m/z 1030.83, 883.71, 736.59, and 589.48, which were assigned to $[7\text{M} + \text{H}]^+$, $[6\text{M} + \text{H}]^+$, $[5\text{M} + \text{H}]^+$, and $[4\text{M} + \text{H}]^+$, respectively, as shown in Figure 1.⁶ The

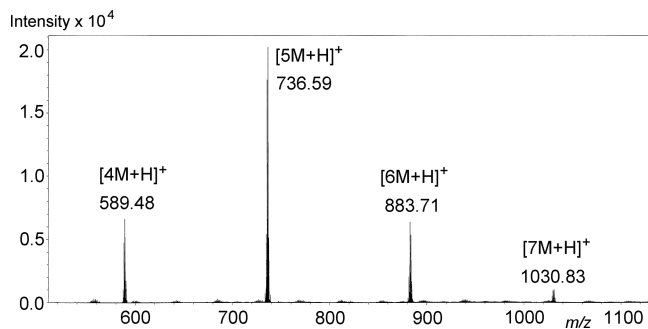


Figure 1. ESI-MS spectrum of **1** in THF in the presence of LiCl in positive ion mode.

observed and theoretical isotopic distributions of each fragment were in close agreement. VPO was performed to estimate the average aggregate size of the compounds. Various concentrations of **1** in benzene (from 0.025 to 0.114 mol dm^{-3}) at 60 °C, in chloroform (from 0.009 to 0.087 mol dm^{-3}) at 40 °C, and in THF (from 0.023 to 0.105 mol dm^{-3}) at 45 °C provided values of 5.7, 5.4 and 5.3, respectively. In each experiment, the VPO plots showed a linear relation ($r = 0.996$ – 0.999) between the concentration and electrical differential within experimental error. The results of the NMR, ESI-MS, and VPO data strongly suggest the presence of aggregates of both 1_5 and 1_6 .

The 2D ^1H – ^1H NOESY spectrum of **1** in CDCl_3 displayed NOEs between H-2 and H-6 of the pyridine moiety and protons of the ethyl groups, and the ^{11}B NMR spectrum of **1** displayed a strong signal at –0.425 ppm (Figures S3 and S4 in the Supporting Information, respectively), showing that the monomer–oligomer equilibrium was exclusively shifted to the side of the oligomer.⁷ These data clearly indicate that **1** assembles mainly into a cyclic pentamer and hexamer that coexist in solution at an approximately 1:1 molar ratio according to the integration values of each corresponding ^1H NMR signal (vide infra). However, the molar ratios of the two oligomers were found to differ depending on the column chromatography fractions from which the samples were derived, the crystallization solvent used, and so on. Therefore,

it was considered that the equilibrium between these oligomers was sufficiently slow at ambient temperature, which was in marked contrast to the thermally equilibrated cyclic oligomers of compound **3**.^{3b}

Structure in the Crystalline State. The structures of the oligomers of **1** were unambiguously determined by X-ray crystallographic studies. Through the slow diffusion of ethanol vapor into a THF solution of compound **1**, we successfully obtained colorless single crystals that were suitable for an X-ray crystallographic analysis.⁸ Crystallization at 7 or 20 °C afforded the cyclic hexamer incorporating one THF molecule ($1_6 \cdot \text{THF}$) in the triclinic crystal system (Figure 2 and Figures S8 and S11

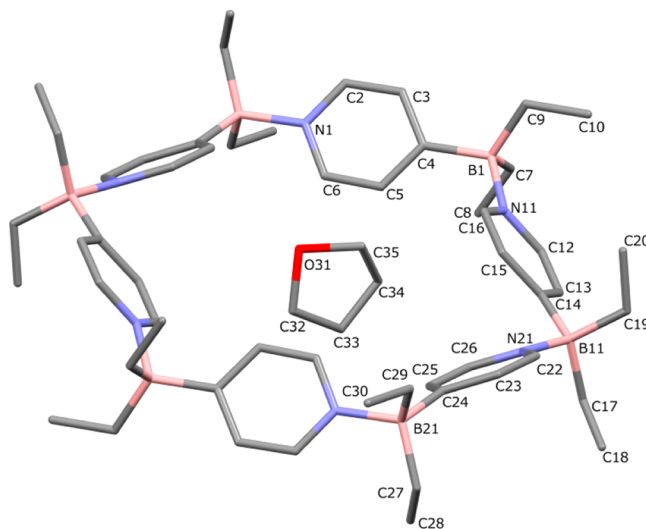


Figure 2. Crystal structure of a hexamer of **1** bearing a THF molecule ($1_6 \cdot \text{THF}$). H atoms and THF molecules disordered over the 2-fold axis are omitted for clarity. Color codes: B (pink), C (gray), N (blue-gray), O (red). The crystallization was performed at 7 °C in THF by vapor diffusion of EtOH.

in the Supporting Information) or in the trigonal crystal system (Figure 3 and Figures S9 and S12 in the Supporting Information), respectively, which were polymorphic. The crystal data and crystallographic refinement parameters of $1_6 \cdot$

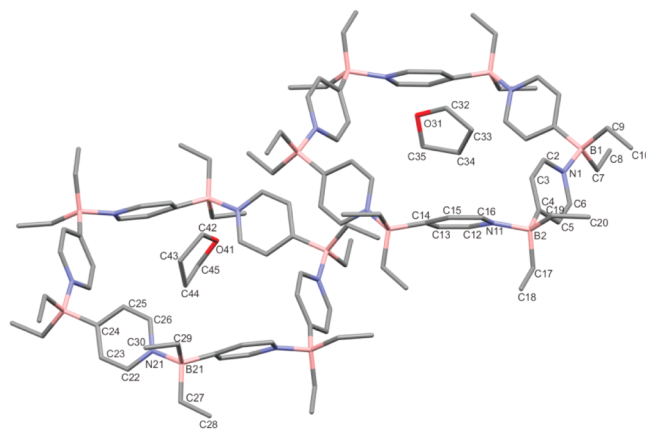


Figure 3. Crystal structure of a hexamer of **1** bearing a THF molecule ($1_6 \cdot \text{THF}$). H atoms and THF molecules disordered over the 3- (right) or 6-fold (left) axis are omitted for clarity. Color codes: B (pink), C (gray), N (blue-gray), O (red). The crystallization was performed at 20 °C in THF by vapor diffusion of EtOH.

THF crystallized at 7 °C are summarized in Table S1 in the Supporting Information, and the selected bond distances and bond angles are listed in Table 1. Another crystal of $I_6 \cdot THF$

Table 1. Selected Geometric Properties of $I_6 \cdot THF^a$

Bond Lengths (Å)			
B1–C4	1.611(4)	B11–C19	1.617(4)
B1–C7	1.634(3)	B11–N21	1.648(4)
B1–C9	1.620(4)	B21–C24	1.626(4)
B1–N11	1.632(3)	B21–C27	1.635(4)
B11–C14	1.621(4)	B21–C29	1.637(5)
B11–C17	1.628(4)	B21–N1a ^b	1.626(4)
Bond Angles (deg)			
C4–B1–C7	106.60(19)	C17–B11–C19	110.7(2)
C4–B1–C9	113.1(2)	C17–B11–N21	105.6(2)
C4–B1–N11	108.84(19)	C19–B11–N21	112.4(2)
C7–B1–C9	112.5(2)	C24–B21–C27	107.0(2)
C7–B1–N11	111.05(17)	C24–B21–C29	110.4(3)
C9–B1–N11	104.9(2)	C24–B21–N1a ^b	109.05(18)
C14–B11–C17	112.5(2)	C27–B21–C29	113.7(2)
C14–B11–C19	107.9(2)	C27–B21–N1a ^b	110.3(3)
C14–B11–N21	107.8(2)	C29–B21–N1a ^b	106.3(2)

^aCrystallization was performed in THF by vapor diffusion of EtOH at 7 °C. ^bN1 atom of the symmetry-related molecule ($-x, 2 - y, 1 - z$).

obtained at 20 °C includes two crystallographically independent cyclic hexamers with different symmetry, and the crystal data and crystallographic refinement parameters are summarized in Table S2 in the Supporting Information. The noteworthy intermolecular interaction for both hexamer·THF complexes crystallized at different temperatures appears to be the CH/ π interaction directed from the CH groups of the THF molecule to the pyridine ring. The shortest interactions between a THF carbon atom and its closest C=C (bond midpoint) of the pyridine ring were found to be 2.93 Å (C34⋯(C15=C16)) for $I_6 \cdot THF$ crystallized at 7 °C and 3.22 Å (C33⋯(C2=C3) and C43⋯(C25=C26)) for $I_6 \cdot THF$ crystal-

lized at 20 °C. The CH/ π interaction, as well as van der Waals contact, would play a dominant role in the host–guest complexation and crystal packing.

As in the case of a THF solution, a $CHCl_3$ solution of **1** at 10 °C furnished the cyclic hexamer bearing some chloroform molecules as single crystals (Figure 4 and Figure S13 in the Supporting Information),⁸ and the crystal data and crystallographic refinement parameters are summarized in Table S3 in the Supporting Information. The crystal of the chloroform complex of **1** consists of two crystallographically independent hexamer-chloroform complexes, (hexamer)₁·(chloroform)₁ and (hexamer)₁·(chloroform)₂, yielding an overall composition of (hexamer)₂·(chloroform)₃. In the (hexamer)₁·(chloroform)₁ complex, the center of the cavity was filled with disordered chloroform molecules over the 6-fold axis. The (hexamer)₁·(chloroform)₂ complex should include a set of chloroform molecules with full occupancy, which corresponds to two such species perching on the hexamer from the upper and lower sides of the cavity, to fill the space between the hexamer layers of the crystal. In addition, the six carbon–chlorine bonds of the two chloroform molecules point toward the faces of the pyridine ring with a distance of 3.790 Å between either chlorine and the center of pyridine ring. Accordingly, the Cl/ π interaction, an attractive dispersion interaction that is sometimes observed in protein–ligand complexes,⁹ appears to attract the chloroform molecules to the hexamers. Packing analysis revealed that these two complexes are alternately arranged on the 3-fold helical alignment along the *c* axis, giving two pitches in a lattice.

On the other hand, quite interestingly, a solution of **1** in a mixture of benzene and hexane (2:1) at 12 °C provided a cyclic pentamer including two benzene molecules ($I_5 \cdot C_6H_6$, Figure 5 and Figures S10 and S14 in the Supporting Information),⁸ which indicates that the solvent used for crystallization can control the preference in which the oligomers will be crystallized. The crystal data and crystallographic refinement parameters are summarized in Table S4 in the Supporting Information. In the pentamer-benzene complex, two benzene

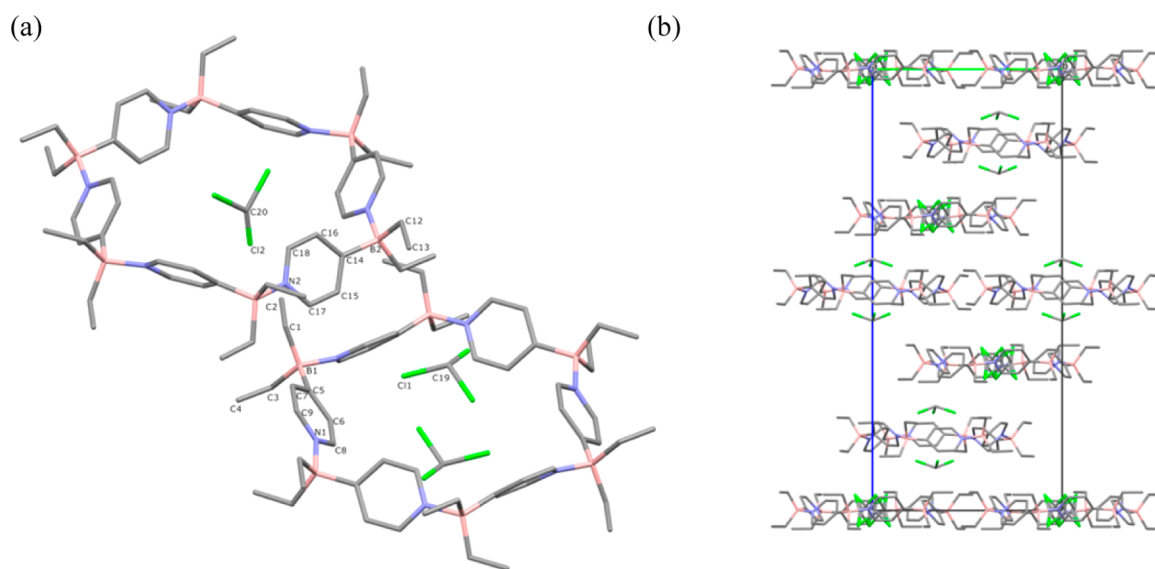


Figure 4. Crystal structure of a hexamer of **1** bearing some chloroform molecules ($I_6 \cdot CHCl_3$). (a) Stick style. H atoms and $CHCl_3$ molecules disordered over the 6-fold axis inside the left hexamer are omitted for clarity. (b) Packing diagram. Color codes: B (pink), C (gray), N (blue-gray), Cl (green). The crystallization was performed at 10 °C in $CHCl_3$.

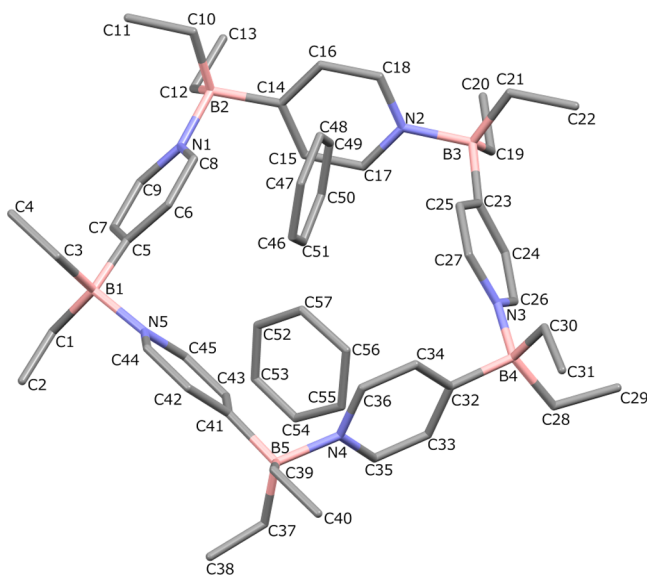


Figure 5. Crystal structure of a pentamer of **1** bearing two benzene molecules ($1_5 \cdot C_6H_6$). H atoms are omitted for clarity. Color codes: B (pink), C (gray), N (blue-gray). The crystallization was performed at 12 °C in benzene/hexane (2:1).

molecules are arranged almost perpendicular to the mean plane of the cyclic pentamer due to CH/ π interactions between the hydrogen of the benzene molecule and the plane of the pyridine ring with a distance of 3.99–4.22 Å from the carbon atom of the benzene to the center of pyridine. It should be stressed that the cyclic oligomers of **1** possess cavities large enough to accommodate small organic molecules; thus, **1** can form inclusion complexes in different ways, depending on the solvent used for crystallization.

The distance between the boron atom and nitrogen atom in the four crystals is in the range of 1.620–1.648 Å, which is almost the same as that of the cyclic tetramer of compound **2** (1.638 Å).^{3a} The bond angles constituted by the boron atom and the three substituents enable calculation of the tetrahedral character (THC) of the boron atom as proposed by Toyota and Ōki.¹⁰ The THC value for **1** in the four crystals is estimated to be 84–92%, which is slightly higher than that of **2** (82%).^{3a} Therefore, the cyclic oligomer of **1** appears to be only slightly more rigid than that of **2**, which might be because the oligomers are tightened by host–guest complexation.

It is noteworthy that either of the two oligomers was predominantly crystallized from the oligomer mixture solution, and that the preference was dependent on the solvent used for crystallization. As the cavity size of the cyclic hexamer of **1** (5.0–5.5 Å) is larger than that of the cyclic tetramer of **2** (1.5–1.7 Å)^{3a} or the cyclic trimer of **3** (~4.0 Å),^{3b} the solvent molecule could be well-accommodated inside the cavity by noncovalent interactions specific to the solvent, which afford a packing diagram suitable for crystallization. It would be difficult for both the cyclic pentamer and hexamer to be arranged in an orderly fashion and form a crystal. The selective crystallization may be explained by the fitness of the size and symmetry between the cyclic oligomer and solvent molecule. Accordingly, the choice of solvent could control the order of preference in which the oligomers would be crystallized. To our knowledge, this is the first report of the selective crystallization of macrocyclic assemblies dependent upon the solvent.

Release of the Incorporated Solvent Molecule. To gain insight into the stability of solvent molecules proximally positioned inside or around the cavity of oligomers of **1**, we performed TGA of the crystals and NMR analysis of the solution. The sample for TGA was prepared by removing the supernatant from the crystal (solid) followed by drying in vacuo. TGA of three solids, the THF complex (crystallized at 7 °C), the chloroform complex, and the benzene complex, upon heating at a rate of 5 °C/min revealed that the weight losses were approximately 7% (70–210 °C), 13% (70–210 °C), and 14% (70–200 °C), respectively, as shown in Figure 6 and

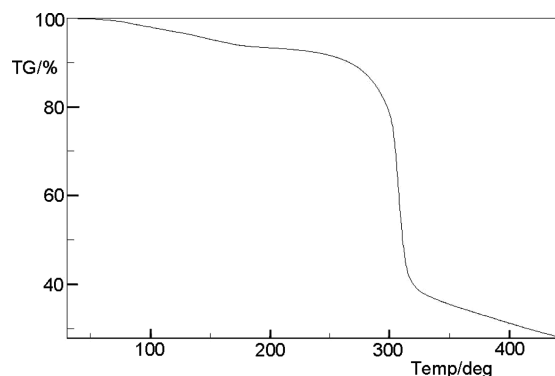


Figure 6. TGA of a THF complex of **1** (crystallized at 7 °C).

Figures S15 and S16 in the Supporting Information. The theoretical weight loss is 7.6% for $1_6 \cdot THF$ (hexamer/THF = 1:1), which is in good agreement with the observed value. However, the theoretical weight losses for $1_6 \cdot CHCl_3$ (hexamer/ $CHCl_3$ = 2:3) and $1_5 \cdot C_6H_6$ (pentamer/ C_6H_6 = 1:2) are 16.9% and 17.5%, respectively, which are larger than the observed values. The solid might contain the solvent adducts of other compositions or solvent-free oligomers. For example, the chloroform complex might contain a 1:1 hexamer- $CHCl_3$ complex (theoretical weight loss of 11.9%) or a pentamer- $CHCl_3$ complex. Although it is difficult to identify such species, these TGA data clearly demonstrate that the solvent molecule included in the macrocycle is released gradually in the temperature range of approximately 70–200 °C. Because this temperature is just slightly higher than the boiling points of the guest solvents, it appears that the guests were not tightly included in the cavity of the macrocyclic host in the crystalline state.

In order to investigate how strongly the cyclic oligomers of **1** can retain the cocrystallized solvent molecules inside or around the cavity in solution, we performed 1H NMR measurements of the THF complex and benzene complex (using identical samples with TGA) dissolved in $CDCl_3$ and of the chloroform complex dissolved in C_6D_6 . The solvent molecules proximally positioned in the crystalline state of the oligomers showed chemical shifts identical to those of the free solvent in 1H NMR spectra (Figures S5, S1, and S6 in the Supporting Information, respectively). This observation indicates that the guest molecule is liberated immediately in solution and replaced by the solvent molecules around it.¹¹ Therefore, it appears that the noncovalent interactions between the host and guest are not strong enough to hold the guest molecule in the cavity in solution.

Assignment of the Cyclic Pentamer and Hexamer in the 1H NMR Spectrum. The single-crystal X-ray analysis

clearly revealed that each compound preferentially obtained from the crystallization solution was a cyclic pentamer or hexamer. However, the solution usually involved a different order of oligomers. In order to separate the pentamers and hexamers, we repeated the column chromatography using silica gel. Unfortunately, this resulted in an incomplete separation. However, when single crystals of $\mathbf{1}_6 \cdot \text{CHCl}_3$ were carefully picked up under a microscope, the pure hexamer¹² was isolated, which can be clearly seen in the ^1H NMR spectrum (Figure S7 in the Supporting Information). The assignment of ^1H NMR signals and a TLC spot originating from the hexamer facilitated the characterization of those from the pentamer. Thus, the set of ^1H NMR signals of pyridyl α - and β -hydrogen in the cyclic oligomers exhibited chemical shifts at 7.94 and 7.24 ppm for the pentamer and at 8.00 and 7.26 ppm for the hexamer. The pentamer was slightly less mobile than the hexamer on a TLC plate with hexane as the developing solvent.

CONCLUSIONS

In summary, two distinct oligomeric structures of a cyclic pentamer and hexamer were obtained by the self-assembly of **1** via intermolecular boron–nitrogen coordination bonds. The use of different solvents appears to have affected the crystallization of both cyclic oligomers. Although complete separation of the isomers still requires some effort, one of the oligomeric isomers seems to preferentially precipitate as single cocrystals with the solvent molecules. Thus, it is clear that the cyclic oligomers of **1** possess an inclusion capability and can form a crystalline host–guest complex, which is the first instance identified in the borylpyridine system. The large cavities of the oligomers would be efficient for complexation with small organic molecules mainly through CH/π interactions. It is well-known that cyclodextrins can include a variety of guest molecules, including ions, through weak interactions in water, such as hydrophobic interactions, hydrogen bonds, electrostatic interactions, etc.¹³ The introduction of a polar functional group into the unit molecule may therefore facilitate complexation with diverse guest molecules. In addition, the combination of self-assembly and further derivatization might open a new route to a cage-like molecule with advanced functions, which could selectively encapsulate certain organic molecules or metal ions. Further design and synthetic studies are in progress.

EXPERIMENTAL SECTION

4-(Diethylboryl)pyridine (1). To a solution of *n*-butyllithium (1.9 M in hexane, 7.7 mL, 14.6 mmol) in ether (30 mL) was added a solution of 4-bromopyridine (2.124 g, 13.4 mmol) in ether (15 mL) at -78°C for 8 min. After 1 h of stirring at the same temperature, a 1 M THF solution of diethylmethoxyborane (26 mL, 26 mmol) was added over 20 min. The mixture was gradually warmed to 0°C over 1 h and stirred for 1 h. The reaction mixture was poured into water (30 mL) and extracted with ethyl acetate (100 mL, 30 mL). The organic layer was washed with brine, dried over MgSO_4 , and concentrated. The crude product was subjected to column chromatography using silica gel (15 g) and benzene/hexane (1:1) as eluent to afford **1** (1.350 g, 68%) as a colorless solid. Mp: $>200^\circ\text{C}$ (lit.⁵ mp $>300^\circ\text{C}$). ^1H NMR (400 MHz, CDCl_3 , δ): benzene complex, 0.50–0.58 (m), 0.62–0.80 (m), 7.24 (d, $J = 6.4$ Hz), 7.26 (d, $J = 6.4$ Hz), 7.36 (s), 7.94 (d, $J = 6.4$ Hz), 8.00 (d, $J = 6.4$ Hz). ^{13}C NMR (100 MHz, CDCl_3 , δ): 9.2, 9.3, 13.8, 14.7, 128.3, 129.0, 142.2, 142.3. ^{11}B NMR (192 MHz, CDCl_3 , δ): -0.425 . IR (KBr): benzene complex, 3446 (br), 2943, 2905, 2866, 2820, 1618, 1424, 1167 cm^{-1} . EIMS (20 eV): m/z 147 (M^+ , 60%), 118 ($\text{M}^+ - \text{Et}$, 100%). HRMS (EI): m/z calcd for $\text{C}_9\text{H}_{14}\text{BN}$ 147.12193,

found 147.12205. ESI-MS (LiCl, THF): m/z calcd for $[(\text{C}_9\text{H}_{14}\text{BN})_7\text{H}]^+$ 1030.86, found 1030.83; calcd for $[(\text{C}_9\text{H}_{14}\text{BN})_6\text{H}]^+$ 883.74, found 883.71; calcd for $[(\text{C}_9\text{H}_{14}\text{BN})_5\text{H}]^+$ 736.62, found 736.59; calcd for $[(\text{C}_9\text{H}_{14}\text{BN})_4\text{H}]^+$ 589.50, found 589.48. Anal. Calcd for $\text{C}_{58}\text{H}_{92}\text{B}_6\text{N}_6\text{O}$ (hexamer·THF complex): C, 73.00; H, 9.72; N, 8.81. Found: C, 72.95; H, 9.53; N, 9.10.

Vapor Pressure Osmometry Results for 1. The sample, purified by column chromatography with benzene/hexane (1:1) as eluent, was used for VPO. The ^1H NMR analysis revealed that the product consisted of **1** (92.6%) and benzene (7.4%). **5.7** in benzene at 60°C [benzil (79, 290, 593, 1073 for 0.0056, 0.021, 0.041, 0.075 mol dm^{-3} , respectively); **1** (54, 97, 165, 279 for 0.025, 0.041, 0.068, 0.114 mol dm^{-3} , respectively)]; **5.4** in chloroform at 40°C [benzil (92, 321, 663, 1198 for 0.0069, 0.025, 0.049, 0.090 mol dm^{-3} , respectively); **1** (46, 56, 154, 234 for 0.009, 0.015, 0.052, 0.087 mol dm^{-3} , respectively)]; **5.3** in THF at 45°C [benzil (127, 340, 612, 1060 for 0.0054, 0.021, 0.042, 0.076 mol dm^{-3} , respectively); **1** (33, 89, 148, 245 for 0.023, 0.038, 0.063, 0.105 mol dm^{-3} , respectively)].

ASSOCIATED CONTENT

Supporting Information

The Supporting Information is available free of charge on the ACS Publications website at DOI: 10.1021/acs.joc.5b02886.

General methods and ^1H , ^{13}C , and ^{11}B NMR, NOESY spectra of **1**, and X-ray crystallographic details and TGA for **1** (PDF)

Crystallographic data of $\mathbf{1}_6 \cdot \text{THF}$ (crystallized at 7°C) (CIF)

Crystallographic data of $\mathbf{1}_6 \cdot \text{THF}$ (crystallized at 20°C) (CIF)

Crystallographic data of $\mathbf{1}_6 \cdot \text{CHCl}_3$ (CIF)

Crystallographic data of $\mathbf{1}_5 \cdot \text{C}_6\text{H}_6$ (CIF)

AUTHOR INFORMATION

Corresponding Author

*E-mail: s-waka@suzuka-u.ac.jp.

Notes

The authors declare no competing financial interest.

ACKNOWLEDGMENTS

We are grateful to Professors T. Murafuji (Yamaguchi University) and K. Takakura (Suzuka National College of Technology) for performing the preliminary studies. We also acknowledge Professors T. Kitagawa and M. Shimizu (Mie University) for their valuable discussion and Dr. K.-I. Oyama and Mr. Y. Maeda (Nagoya University) for their help with the EIMS, CSI-MS, elemental analysis, and ^{11}B NMR spectroscopy. The crystal structures of $\mathbf{1}_6 \cdot \text{THF}$ (crystallized at 7°C), $\mathbf{1}_6 \cdot \text{THF}$ (crystallized at 20°C), $\mathbf{1}_6 \cdot \text{CHCl}_3$, and $\mathbf{1}_5 \cdot \text{C}_6\text{H}_6$ were deposited at the Cambridge Crystallographic Data Centre with the deposition numbers CCDC 1441651, 1441547, 1441985, and 1441650, respectively.

REFERENCES

- (1) (a) Cragg, M. L. *Organoboranes in Organic Synthesis*; M. Dekker: New York, 1973. (b) Brown, H. C. *Organic Synthesis via Boranes*; John Wiley & Sons, Inc.: New York, 1975. (c) Negishi, E. J. *Organomet. Chem.* **1976**, *108*, 281–324. (d) Miyaura, N.; Suzuki, A. *Chem. Rev.* **1995**, *95*, 2457–2483.
- (2) (a) Hodgkins, T. G.; Powell, D. R. *Inorg. Chem.* **1996**, *35*, 2140–2148. (b) Barba, V.; Höpfl, H.; Farfán, N.; Santillan, R.; Beltran, H. I.; Zamudio-Rivera, L. S. *Chem. Commun.* **2004**, 2834–2835. (c) Christinat, N.; Scopelliti, R.; Severin, K. *Chem. Commun.* **2008**, 3660–3662.

- (3) (a) Sugihara, Y.; Takakura, K.; Murafuji, T.; Miyatake, R.; Nakasuji, K.; Kato, M.; Yano, S. *J. Org. Chem.* **1996**, *61*, 6829–6834. (b) Wakabayashi, S.; Sugihara, Y.; Takakura, K.; Murata, S.; Tomioka, H.; Ohnishi, S.; Tatsumi, K. *J. Org. Chem.* **1999**, *64*, 6999–7008. (c) Wakabayashi, S.; Imamura, S.; Sugihara, Y.; Shimizu, M.; Kitagawa, T.; Ohki, Y.; Tatsumi, K. *J. Org. Chem.* **2008**, *73*, 81–87. (d) Wakabayashi, S.; Kuse, M.; Kida, A.; Komeda, S.; Tatsumi, K.; Sugihara, Y. *Org. Biomol. Chem.* **2014**, *12*, 5382–5387.
- (4) (a) Fujita, M.; Umemoto, K.; Yoshizawa, M.; Fujita, N.; Kusukawa, T.; Biradha, K. *Chem. Commun.* **2001**, 509–518. (b) Fujita, M.; Tominaga, M.; Hori, A.; Therrien, B. *Acc. Chem. Res.* **2005**, *38*, 369–378.
- (5) Ishikura, M.; Mano, T.; Oda, I.; Terashima, M. *Heterocycles* **1984**, *22*, 2471–2474.
- (6) When ESI-MS measurements were carried out in the absence of LiCl, no peaks assignable to oligomers were observed. In the presence of LiCl, the efficiency of $[M + H]^+$ formation was considered to be higher than that of $[M + Li]^+$ formation.
- (7) The boron of **1** is found to resonate at a position far higher than that of a trivalent boron, for example, 1-(dimesitylboryl)-4-(dimethylamino)benzene (71.5 ppm). The marked shielding of the boron in triethylborane-trimethylamine adduct (–0.1 ppm) and trimethylborane-pyridine adduct (0.0 ppm) has been determined to be due to the coordination bond between the trivalent boron and the nitrogen of amines. See: (a) Nöth, H.; Vahrenkamp, H. *Chem. Ber.* **1966**, *99*, 1049–1067. (b) Nöth, H.; Wrackmeyer, B. *Chem. Ber.* **1974**, *107*, 3070–3088 and ref 3.
- (8) A solution of **1** (~50 mg) in solvent (3 mL) was allowed to stand at the stated temperature and was slowly evaporated to afford the crystal solid. Although the ratios of the two oligomers in the solid were different depending on the sample lot, even in the same solvent, no alternation of the crystal structure was observed at all.
- (9) Imai, Y. N.; Inoue, Y.; Nakanishi, I.; Kitaura, K. *Protein Sci.* **2008**, *17*, 1129–1137.
- (10) Toyota, S.; Ōki, M. *Bull. Chem. Soc. Jpn.* **1992**, *65*, 1832–1840.
- (11) CSI-MS is effective for analyzing the solution structure of metal complexes: Yamaguchi, K. *J. Mass Spectrom.* **2003**, *38*, 473–490 We attempted to observe the THF complex of hexamer in a THF solution by means of CSI-MS, but this afforded only the peaks for the pentamer, hexamer, and heptamer, with no THF molecule.
- (12) While the isolated hexamer was put in $CDCl_3$ at ambient temperature for six days, NMR spectra remained unchanged, indicating that the transformation to the pentamer did not occur. Therefore, each oligomer appears to be relatively stable at ambient temperature, which is consistent with the consideration mentioned in the section of NMR spectroscopy.
- (13) (a) Saenger, W. *Angew. Chem., Int. Ed.* **1980**, *19*, 344–362. (b) Harata, K. *Chem. Rev.* **1998**, *98*, 1803–1828.